SAND2014-15513C

Prediction of Spatial Distributions of Equilibrium Product Species from High Explosive Blasts in Air

Aaron L. Brundage[1] and Stephen W. Attaway[2] and Michael L. Hobbs[3]
Michael J. Kaneshige[4] and Lydia A. Boye[5]
Sandia National Laboratories, Albuquerque, NM, 87185

Blast waves from an explosion in air can cause significant structural damage. As an example, cylindrically-shaped charges have been used for over a century as dynamite sticks for mining, excavation, and demolition. Near the charge, the effects of geometry, standoff from the ground, the proximity to other objects, confinement (tamping), and location of the detonator can significantly affect blast wave characteristics. Furthermore, nonuniformity in the surface characteristics and the density of the charge can affect fireball and shockwave structure. Currently, the best method for predicting the shock structure near a charge and the dynamic loading on nearby structures is to use a multidimensional, multimaterial shock physics code. However, no single numerical technique currently exists for predicting fireball combustion, especially when particulates from the charge are propelled through the fireball and ahead of the leading shock lens. Furthermore, the air within the thin shocked layer at temperatures above an electron volt can dissociate and ionize. Hence, an appropriate equation of state for air is needed in these extreme environments. As a step towards predicting this complex phenomenon, a technique was developed to provide the equilibrium species composition at every computational cell in an air blast simulation as an initial condition for hand-off to other analysis codes for combustion fluid dynamics or radiation transport. Here, a bare cylindrical charge of TNT detonated in air is simulated using CTH, an Eulerian, finite volume, shock propagation code developed and maintained at Sandia National Laboratories. The shock front propagation is computed at early times, including the detonation wave structure in the explosive and the subsequent air shock up to 100 microseconds, where ambient air entrainment is not significant. At each computational cell, which could have TNT detonation products, air, or both TNT and air, the equilibrium species concentration at the density-energy state is computed using the JCZS2i database in the thermochemical code TIGER. This extensive database of 1439 species, including 192 ions, can predict thermodynamic states up to 20,000 K. The results of these calculations provide the detailed three-dimensional structure of a thin shock front, with a thickness on the order of 0.1 cm, and spatial species concentrations including free radicals and ions. Furthermore, air shock predictions are compared with experimental pressure gage data from a right circular cylinder of pressed TNT, detonated at one end. These complimentary predictions show excellent agreement with the data for the primary wave structure.

Nomenclature

C_s = sound speed
C_V = specific heat at constant volume
E = internal energy
E_H = Hugoniot internal energy
M = reaction rate parameter

[1] Principal R&D Scientist, Integrated Military Systems Development Center, P.O.Box 5800, MS 1160, AIAA Member.
[2] Distinguished R&D Scientist, Engineering Sciences Center, P.O.Box 5800, MS 840.
[3] Principal R&D Scientist, Department Name, Engineering Sciences Center, P.O.Box 5800, MS 836.
[4] Distinguished R&D Scientist, Energetic Components Center, P.O.Box 5800, MS 1454, and AIAA Senior Member.
[5] Distinguished R&D Scientist, Systems Research Center, P.O.Box 5800, MS 1207.

P = pressure
P_H = Hugoniot pressure
P_I = threshold pressure of initiation
P_R = reaction pressure
P_{RP} = pressure of reaction products
s_1, s_2 = coefficients in shock velocity Hugoniot relationship
U_s = shock velocity
X, Y = coordinate directions
z = compressibility, reaction rate parameter
ϕ = history variable
Γ_0 = Grüneisen coefficient
λ = extent of reaction
μ = volumetric strain
ρ_0 = initial density
ρ = density
τ_0 = time constant

I. Introduction

THE detonation of confined explosives in air or inert test chamber environments provides a unique opportunity to study both combustive effects and blast-structure interactions. There are many applications which would benefit from basic and applied research in this area, such as studies of blast effects near a high explosive (HE) charge, or on surrounding structures or human assets;[1] industrial hazard analyses or accident scenarios,[2] and advancing the state-of-the-art in air-breathing propulsion for improving pulse detonation engine technology.[3] Carefully planned model validation studies, where the experiments are designed to provide data for computational model assessments, can be used to ultimately improve predictive model capability, providing a much needed basis of confidence, particularly for predicting fireball structure and evolution from a high explosive detonation. Here, a condensed HE is shock initiated, where reaction in the material, or decomposition to stable chemical condensed species such as C or gaseous species such as CO, H_2O, CO_2, N_2, etc. occurs over a short run distance, leading to the transition from the input shock load to a detonation. This steady detonation wave, or a self-supported reactive shock, propagates at a constant velocity through the HE until it interacts with the surrounding fluid at the edge of the explosive. If this material is air, for example, the air is rapidly compressed, producing an air shock that initially ionizes for temperatures exceeding 9000 K. The leading air shock propagates downstream, preheating the air ahead of it, and creating release states in the detonation products behind it. Eventually, vacuum conditions are created behind the shock, and a recompression shock is formed. According to optical measurements, turbulent mixing of the air and detonation products becomes significant beyond 100 us, producing a fireball that initially moves at the same velocity as the leading air shock.

This process of producing a detonation wave structure, and the late-time mixing of the detonation products with entrained air to produce a flame front, or fireball, is shown schematically in Fig. 1. Details on describing this process can be found in numerous texts.[4,5,6] The term Hugoniot is defined as the locus of end states, assuming a steady flow process that conserves mass, momentum, and energy, due to a single shock from an initial state. The end state is connected to the initial state via the Rayleigh line. Following the ZND theory of detonation, the detonation wave structure consists of a thin reaction zone, defined by states B and C in Fig. 1, where state B identifies the location where chemical reactions

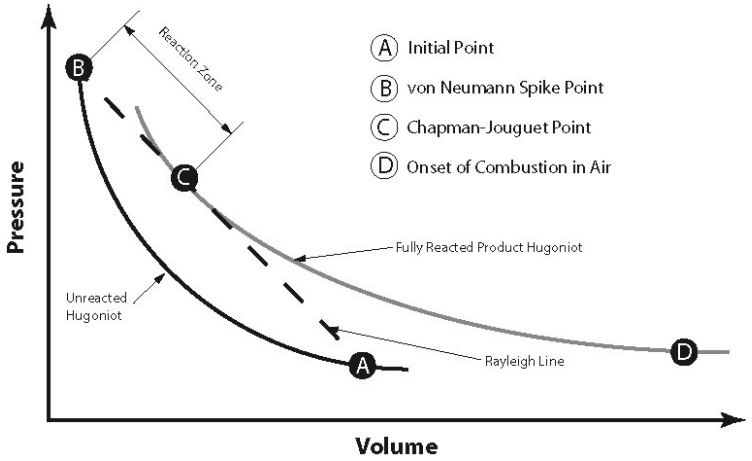

Figure 1. Various thermodynamic pressure-volume states, and the relationship between the unreacted and reacted product Hugoniot curves during detonation.

start (the von Neumann spike) and state C represents the sonic point, or Chapman-Jouguet (CJ) point, marking the end of the reaction zone. Since states A, B, and C are all connected by the same Rayleigh line, the detonation shock wave and burn front given by the end of the reaction zone move at the same CJ detonation velocity. After the CJ state, the detonation products expand to large volumes. For explosives in air, the interaction of the detonation wave and air at the boundary of the explosive will rapidly compress the air, producing an air shock at sufficiently high temperatures to dissociate and ionize air molecules. At later times, mixing of the air with hot detonation product gases will produce a luminous flame front behind the air shock, given by state D in Fig. 1.

Modeling this process of high explosive detonation to deflagration has been complemented by experiments in a significant multi-year, multi-agency research effort. At this present time, a single computational tool does not exist for modeling the entire explosive event by predicting the multidimensional wave structure at states A through D over times that can last seconds or longer, depending upon the size, composition, and method of initiating the charge.

It has been known for many years that combustion in air from the expansion of hot detonation products is accompanied by a local increase in pressure (due to detonation wave reflections) for confined explosions from high explosive charge detonations.[7] For confined explosions in a bomb calorimeter, measurements of the *heat of combustion* were in excellent agreement with predictions of constant volume expansion using equilibrium chemistry for 25g-TNT charges in air.[8] Smaller, 1g-TNT charges were also initiated in sealed tunnels with air or nitrogen environments, where the wall pressure was measured along the tunnel length from the transit of blast waves. Spatial distributions of the mean shock overpressure from the static gages were compared with thermodynamic predictions of constant volume expansion at a single state using equilibrium chemistry calculations. This approach was shown to be inadequate for predicting the mean overpressure distribution. In subsequent reporting, a turbulent combustion model was introduced, where the flowfield was initialized by a spherical wave at the CJ state and equilibrium composition.[9] With this methodology, the actual charge geometry and the spatial distribution of chemical equilibrium species corresponding to the CJ detonation wave structure were not considered. With this method of initialization, the products are at the CJ temperature. The air shock, which could be at a significantly higher temperature with dissociated or ionized species, is not represented. Hence, the impedance mismatch between the explosive and air is ignored. Assuming infinitely fast mixing of the fuel and air in an invsicid flowfield, afterburning of the detonation products in air behind the blast wave were predicted. For gram-sized aluminized explosive charges initiated as part of the same small-scale chamber test series, Newald presented electrical conductivity measurements of the detonation products cloud. In the single snapshot provided, the blast wave was shown to be ahead of the luminous flame front. Knowing the temporal and spatial evolution of the detonation product combustion from experiments would provide useful insight to complementary numerical studies for when ignition occurs and the flame front separates from the blast wave. This information could be used to determine at what time a simulated spatial species field should be handed to a combustion fluid dynamics code.

Larger, 440-493 g-spherical charges of TNT and PBX9404, which were initated in the center or on top in several environments, each having a different level of oxygen content (including air), were experimentally investigated to quantify the influence of detonation product afterburn.[10] The fireball radius as a function of time was measured photometrically and radiometrically. A one-dimensional Lagrangian hydrocode was used to predict the shock wave propagation in the air following the TNT and PBX9404 charge detonations. Mixing was not included in the shock simulations, and after 200 μs, when turbulent mixing between the detonation products and air was shown to be significant for a fireball radius exceeding 10 times the initial charge radius, the fireball radii became increasingly underpredicted. Oxidation occurs during this secondary combustion process such that some solid carbon C(c) and CO, for example, are converted to CO_2, and some H_2 is converted to H_2O. By comparing radiometric data for different oxygen atmospheres, the magnitude of the radiative flux increases with increasing oxygen content, and the peak flux shifts to later times, demonstrating a strong influence of afterburn on radiation. Accordingly, the radiative flux profiles in the 2.2 μm spectral band began at 100 μs for the air and predominatly N_2 atmospheres, where afterburning began at 10 μs for the predominantly O_2 atmosphere. Furthermore, the location of the detonator affects the radiative signature, with the top initiated sphere having more than three times the peak intensity than the center detonated one. Since radiometric measurements are highly temperature dependent, the shock focusing from the off-center detonator placement creates regions of elevated temperature and a non-spherical detonation wave structure. This would suggest that the onset of afterburning chemistry is dominated by radiation, and it occurs prior to significant turbulent mixing between the air and fuel. Photographic measurements of the fireball radius demonstrate cycles of fireball contraction and expansion, driven by shock recompression and reflection, at much later times in excess of 800 μs. When the fireball temporarily stops expanding, before beginning to contract, the leading blast wave continues to propagate in the same direction, breaking away from the fireball. Thus, any combustion fluid

dynamics tools used to model detonation product secondary combustion should also be able to resolve complex shock interactions.

This paper highlights the unique advances in the tools that were required to produce three-dimensional field data of the local thermodynamic state variables and equilibrium species concentrations following the detonation of a cylindrical charge of TNT in air. The cylindrical charge, detonated on one end, produced a highly nonuniform detonation wave profile; hence, the shock to detonation transition (SDT) and the thin reaction zone were captured within the explosive, and the development of the air shock and the blast wave propagation were modeled at later times. Thermochemical equilibrium codes do not compute shocks or track the velocity of materials. For detonations from ideal explosives, it is assumed that the chemical reactions will run to completion and the detonation products will be in equilibrium. Thus, a new tool interfacing separate codes for both the shock physics and equilibrium chemistry was developed to provide a spatial distribution of species for a given shock wave profile. The format of the resulting large data sets and the time that they are interfaced with a combustion fluid dynamics code are discussed. Based upon a review of literature presented herein, there was not a precedent for simulation of condensed phase CHNO molecular high explosives detonation coupled with the production of ionizing air shocks in multidimensions and subsequent deflagration of the hot detonation products. Previous numerical studies aimed at predicting afterburn were shown to be strongly dependent on initial conditions. Using a single computational tool such as an equilibrium chemistry code, a combustion fluid dynamics code, or a hydrocode to model secondary combustion were all shown to be inadequate; hence, an integrated method that integrates all three tools is necessary given the wide range of time scales, length scales, and physical processes that drive disparate numerical methods.

II. Methodology for Linking a Shock Physics Code to an Equilibrium Chemistry Solver

The high explosive detonations and air shock propagation results presented herein were computed with CTH,[11] a multidimensional, multimaterial Eulerian shock physics code developed and maintained by Sandia National Laboratories for modeling large deformations or strong shock problems. Material models within CTH treat material strength, fracture, and porosity. These models are based on a combination of equations of state (EOS) and yield strength models for treating shear behavior. The EOS models treat most states of matter found in shock physics. By using the appropriate material models, phenomena such as melting, vaporization, and explosive burns or detonations can be simulated. The availability of large parallel computer platforms and development of adaptive mesh refinement within CTH have dramatically improved the ability to run simulations at very high resolutions for a wide variety of problems.

TIGER[12] is a thermochemical equilibrium code used for condensed and gas phase detonation calculations. Detonation properties and shock Hugoniots are computed with the JCZ3 equation of state using parameters from the JCZS EOS database of product species and ions developed at Sandia National Laboratories by Hobbs et al.[13] The database was recently expanded to include over 1400 species with nearly 200 ions, and to be valid over an extended range of temperatures up to 20,000 K. Since high explosive detonations in air can produce air shocks in excess of 10,000 K, the revisions of the database, as documented by Hobbs et al, were needed to predict gas phase product species within an air shock.

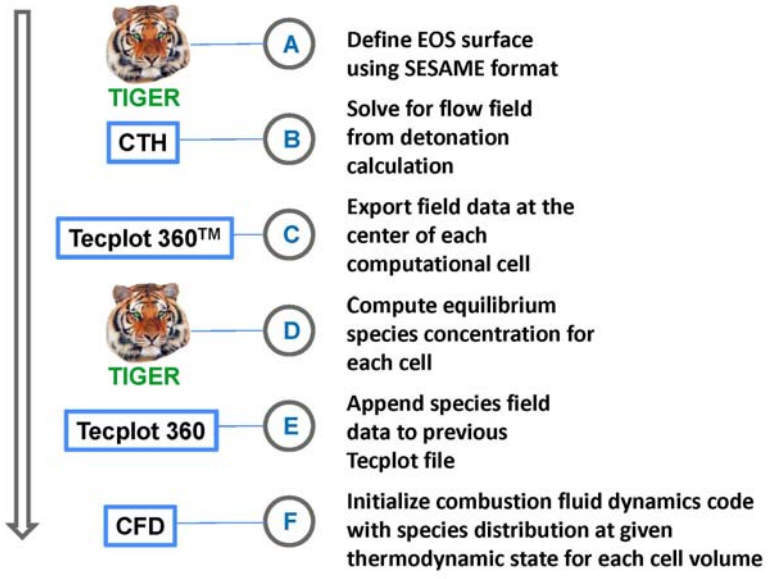

Figure 2. Methodology for using CTH-TIGER to create spatial species concentration for each thermodynamic state at computation cell centers for interfacing with a computational fluid dynamics code.

A major outcome of this paper was to develop a methodology for linking CTH with TIGER to produce

a set of initial conditions for CFD, and to provide a dataset for model validation. The six-step process for CFD initialization is given in Fig. 2. In the first step (*A*), the JCZ3 EOS in TIGER is used with the JCZS2i database to create tabular equations of state for the detonation products and the air. These equations of state are converted to SESAME[14,15] format for use in CTH. These tables provide pressure and internal energy as functions of density and temperature, and a default reference state. Most SESAME tables also have accompanying reference documentation. For the second step (*B*), CTH is used to compute the shock wave propagation through each material from the initiation of the high explosive. With a tabular EOS, shock and release to a variety of condensed matter states can be achieved. In the third step (*C*), thermodynamic state variables are exported to Tecplot 360™ data files.[16] Data loaders for Tecplot files are openly available; hence, these files can be read and plotted by many applications, making this the file format that was chosen to be shared across CTH, TIGER, and the CFD tool. In the fourth step (*D*), an equilibrium chemistry calculation was completed for each cell-centered value. For the calculations reported herein, this meant TIGER was called for each computational cell in a domain with over a millon cells, leading to numerous improvements to increase efficiency. For the fifth step (*E*), the equilibrium species concentration for up to 20 gaseous and condensed species were appended to the previous Tecplot files, combining them with the thermodynamic state variable data over the entire computational mesh. For massively parallel computations on massively parallel compute platforms, Tecplot files were exported for each processor from CTH, and additional software was written to recombine the appended per processor Tecplot files into a single file upon user request. In the final step (*F*), the Tecplot files were imported by the CFD application.

Hence, this paper documents a new computational tool, CTH-TIGER, which was developed to transition from a detonation to an air shock, and to provide a spatial field including the species and relevant thermodynamic variables to initialize a combustion fluid dynamics code. This represents a significant advancement over the previously reported approach of initializing a CFD code with the CJ state to predict secondary detonation product combustion.

III. Computational and Experimental Results

The following section provides computational results from CTH simulations and complementary experimental results for model assessment. Spatial distributions of species concentrations for shock wave profiles at various snapshots in time, computed with CTH-TIGER in both one and three dimensions are also presented.

A. CTH Reactive Burn Modeling

The CTH software code integrates the conservation equations for mass, momentum, and energy in a two-step solution sequence.[11] The first step of this numerical scheme is a Lagrangian step based on mixed cell pressures that distorts the mesh to track material motion. Finite volume approximations to the Lagrangian conservation equations for momentum and energy are solved over a time step, while mass conservation is trivial since mass flux is not transported across the cell boundaries. During the second step, the mesh is rezoned and the distorted material is advected through a fixed Eulerian mesh using a second order accurate conservative scheme developed by van Leer.[17] Using the equation of state package, thermodynamic variables are updated. Results from one-dimensional cylindrical, two-dimensional cylindrical, and three-dimensional rectangular simulations will be presented in this paper. Adaptive Mesh Refinement (AMR) is available to selectively refine the mesh based upon user-selected indicators for individual state variables, as demonstrated for a subset of the simulations presented herein.

Reactive burn models in CTH are used to predict the ZND detonation wave structure in condensed phase explosives, plastics, or polymers. To resolve the thin reaction zone, a finely zoned mesh is required. The History Variable Reactive Burn (HVRB) model[15] was developed to estimate shock initiation and failure in heterogeneous explosives. This model uses a pressure-based rate law for describing thick-pulse initiation in complicated geometries. The pressure for the partially reacted explosive is expressed in terms of the material density ρ, temperature T, and extent of reaction λ, and comprised of a linear combination of the unreacted pressure P_{UR} and the reacted pressure P_{RP}, as given in Eq. (1).

$$P(\rho, T, \lambda) = (1-\lambda)P_{UR}(\rho, T) + \lambda P_{RP}(\rho, T) \tag{1}$$

The extent of reaction is used in Eq. (1) to transition from an unreacted material ($\lambda = 0$) to a fully reacted material ($\lambda = 1$), achieving states that are bounded by the Hugoniot curves given in Fig. 1. This rate law defining the extent of reaction is given in Eq. (2).

$$\lambda = \min(\phi^M, 1) \tag{2}$$

The history variable ϕ is a dimensionless quantity defined as the integral over time of a kernel based upon cell pressure, as given by Eq. (3).

$$\phi = \tau_0^{-1} \int_0^t \left[\left(P - P_I \right) / P_R \right]^z d\tau \tag{3}$$

The unreacted EOS is defined with the Mie-Grüneisen formula, which is fit to experimental shock Hugoniot data. As given by Eq. (4), the pressure of the unreacted explosive is expressed as a linear relationship between pressure and energy at the Hugoniot reference state, with the assumption of constant specific heat.

$$P_{UR}(\rho, E) = P_H(\rho) + \Gamma_0 \rho_0 \left[E - E_H(\rho) \right] \tag{4}$$

The Rankine-Hugoniot relationships, defined by integrating the conservation equations for mass, momentum, and energy across a steady one-dimensional shock, are given in Eqs. (5) to (7). Additionally, an empirical relationship for the shock velocity U_s is given in Eq. (8). For this equation set, the initial pressure, particle velocity, and energy are assumed to be zero at the initial density and temperature.

$$\mu = 1 - \rho_0 / \rho \tag{5}$$

$$P_H = \rho_0 U_s^2 \mu \tag{6}$$

$$E_H = P_H \mu / (2\rho_0) \tag{7}$$

$$U_s = 2C_s \left[1 - s_1 \mu + \sqrt{(1 - s_1 \mu)^2 - 4 s_2 \mu^2} \right]^{-1} \tag{8}$$

A tabular EOS in SESAME format is used to define the state of the reaction products. For the work reported herein, this format is needed to cover a wide density range, incorporating a variey of physical phenomena such as phase transitions, dissociated and ionized states. Furthermore, SESAME equations of state work best with CTH reactive burn models, and are more accurate than analytical equations of state that only specify the release isentrope, such as the JWL,[18] for computing Taylor wave structure, detonation wave interactions, and release states that are not coincident with the CJ isentrope. With the exception of the time constant τ_0, the HVRB model is fit to data that quantify the run distance (or run time) versus pressure for a steady detonation. The constants given in Eqs. (1) to (8) for fitting an HVRB model to pressed TNT are listed in Table 1.

Table 1. Equation of State Parameters for Pressed TNT Reactive Burn Models in CTH.

ρ_0, g/cc	C_s, cm/s	s_1	s_2	Γ_0	C_V, J/g·K	P_R, kbar	P_I, kbar	z	M	τ_0, s
1.63	2.31×10^5	2.14	0	0.59	1.11	65	5	3.8	1.5	1×10^{-6}

B. Experimental Setup

Experiments were conducted at Sandia National Laboratories Explosive Components Facility (ECF) to determine the behavior of pressed TNT explosives in a controlled environment. Trials were conducted for charges suspended at the center of the ECF test chamber, as shown by the cut-away view in Fig. 3.

A 511 g right cylindrical charge of pressed TNT was initiated on one end by a RISI RP-1 detonator with its tip glued to the surface at the center. Nominally, the charges have a 5 cm diameter and a 4 cm height with a pressed density of between 1.60 and 1.63 g/cc. Pencil pressure gauges were aimed toward the center of the explosive charge, and high speed video recording of the explosive

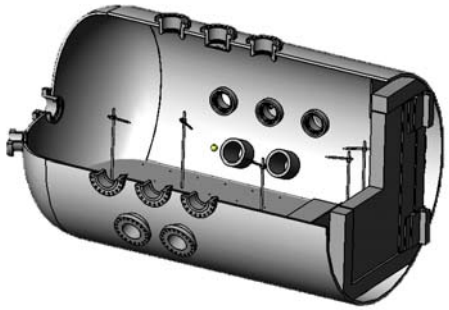

Figure 3. Illustration of the ECF test chamber with a charge located in the center and diagnostics.

event was conducted with a million-frame-per-second HPV-1 Shimadzu camera located at a viewing port. Pressures were measured with PCB (model 137A22) pencil gauges, each having a 500 psi range, a maximum rise time of 4 μs, and a time constant in excess of 0.2 s. The chamber was flooded with air or N_2 to determine the degree of secondary detonation product combustion with excess O_2; however, results are reported herein for air environments.

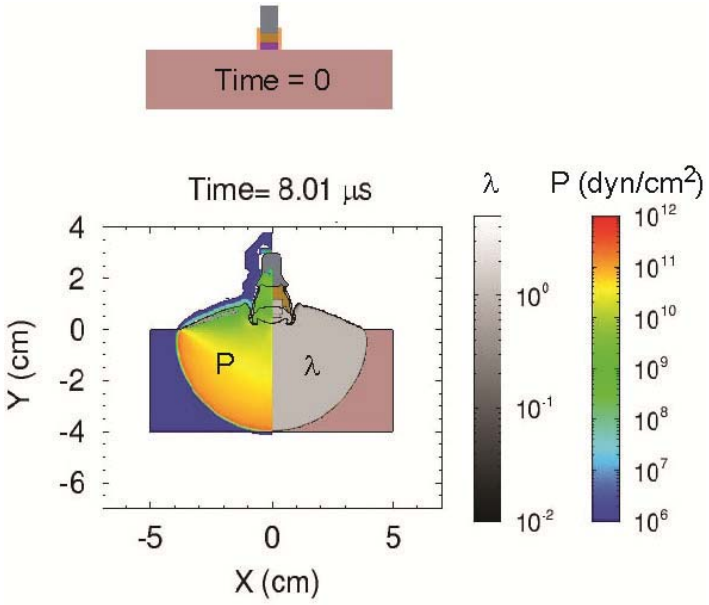

Figure 4. Shock initiation and detonation of a cylindrical charge of TNT predicted with CTH.

C. Experimental Comparisons

The CTH simulations were conducted on Chama, a 392 TFLOP high performance computing platform using 2.6 GHz Intel Sandy-Bridge EP processors (2 sockets, 8 cores/socket), having a total of 1,232 nodes (19,712 cores) and 64 GB of memory per node. The machine runs on a Red Hat Enterprise Linux 6 operating system. CTH calculations were conducted to predict shock initiation and detonation of the TNT charge in air, assuming a two-dimensional axisymmetric geometry, with the axis of symmetry aligned with the major axis of the charge and detonator. The total domain size was 256 cm x 256 cm, using a fixed cell size of 0.025 to 0.125 cm for flat mesh simulations, and a minimum cell size of 0.037 cm for mesh adaptivity with AMR. Up to 16 nodes were used for the computations. The computational setup, which mimics the experiments capturing the RP-1 detonator, pressed TNT charge, and air environment, is shown at the initial time (time = 0) in Fig. 4. The HVRB model for TNT is given in the previous section, and a SESAME EOS for air was constructed from TIGER and converted to a binary file using the CTH code suite. Equations of state for the detonator were constructed using a similar methodology. At a later time of 8 μs, the steady detonation shock wave (depicted by the pressure) propagates the reaction (depicted by the burn front of the fully reacted material at λ = 1).

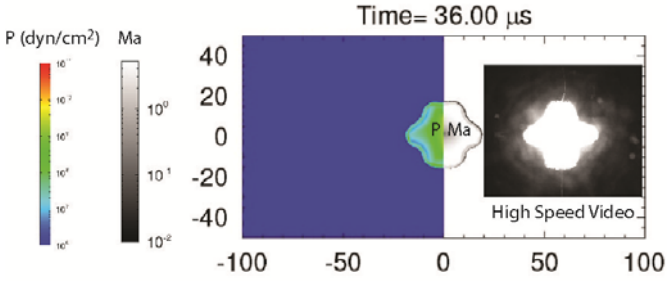

Figure 5. Complex shock structure predicted by CTH and compared with luminous front from high speed video.

At a time of 36 μs, the shape of the shock front in air is shown to match the luminous front recorded by the high speed video in Fig. 5. Including the detonator as part of the model provided a non-uniform input pulse, and use of a reactive burn model with a tabular EOS was needed to capture the two-dimensional detonation wave structure and complex wave interactions leading to the non-uniform shock wave profile. Preheating of the gas ahead of the primary blast wave occurs by radiation heat conduction. In an air shock with a temperature of 10,000 K, the preheating layer is about 0.01 cm,[19] which is a fraction of the cell size used in these

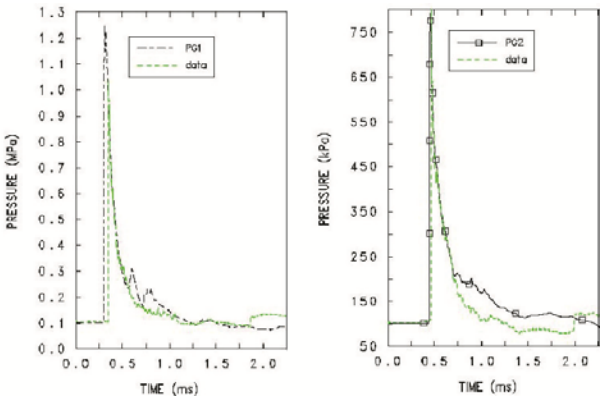

Figure 6. Experimental pressure profiles from gauge records compared with CT H pressure predictions.

computations. This preheating by radiation causes the shock front to glow, allowing tracking of the front by optical methods, and measurement of the emitted radiation over a range of wavelengths.

Pressure gauge records were compared with CTH tracer records at the same locations, as shown in Fig. 6. The pressure gauges were located at 30 cm (PG1) and 35 cm (PG2) from the center of the charge. Generally, the shock wave characteristics such as the peak overpressure, arrival time, decay time, and impulse of the primary wave were well predicted by CTH. These predicted traces were not shifted in time to match the data.

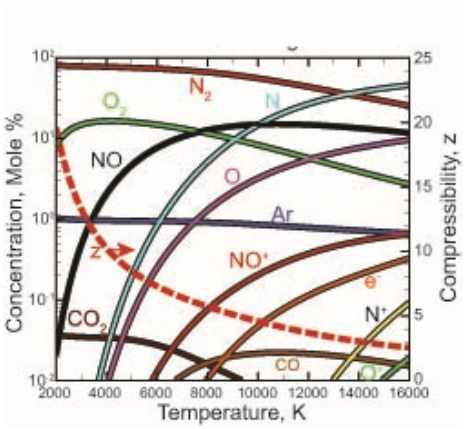

Figure 7. Air composition at 250,000 atm as calculated with the JCZS2i-EOS.

D. 1D CTH-TIGER Predictions

One-dimensional (1D) simulations of an infinitely long TNT cylinder, having a radius of 5 cm and surrounded by air were conducted with CTH. The total domain length was up to 50 cm, and the cell size was 0.01 cm; these simulations were run on a single processor. Using a simplified 1D geometry at high resolution provided adequate resolution of the reaction zone in the detonation wave, and the thin air shock generated at the boundary of the explosive and its subsequent propagation for simulation times up to 100 μs. For the peak overpressure in the thin air shock predicted in the 1D CTH calculations, equilibrium compositions of air were predicted using the JCZS2i database in TIGER, as shown in Fig. 7. The air composition chosen was equivalent to the standard air properties given by the National Bureau of Standards: 78.08% N_2, 20.95% O_2, 0.93% Ar, 0.033% CO_2, and 0.003% Ne. At 250,000 atm, real gas behavior is prevalent at low temperatures, and at higher temperatures, air approaches ideal gas behavior. As demonstrated by Hobbs et al., rarefied air species concentrations were shown to be similar to published data and equivalent to predictions by the NASA-CEA code.[20] These data comparisons, as well as extensive comparisons to detonation velocity data demonstrate the successful validation of TIGER equilibrium predictions.

CTH-TIGER predictions of TNT detonation in air, with profiles of temperature, pressure, and composition at various simulation times, are given in Fig. 8. At 7 μs, the detonation wave is captured in the explosive, and profiles of the species corresponding the wave structure, as given by the pressure and temperature, demonstrate that the major species in the reaction products are C(c), CO, H_2O, H_2, and CO_2. TNT is very fuel rich, and produces significant amounts of solid carbon since there is insufficient oxygen (-74% oxygen balance) available for complete combustion. Since the air has not reacted, its composition remains unchanged. By 8 μs, a thin 600-μm air shock with an elevated temperature of 11,170 K and pressure of 256,000 atm is formed, due to the low shock impedance of air relative to the explosive. Notice that these values are significantly higher than the values at the CJ state (T_{CJ} = 3449 K, P_{CJ} = 190,000 atm). Over time, at 50 and 100 μs, the temperatures remain high with a significant temperature gradient across the shock; however, the pressure has fallen three orders of magnitude. Dissociation and ionization phenomena are highly temperature dependent; hence, these strong temperature gradients will affect the species distribution within the shock.

The species distribution, given by mole % as a function of axial distance, within the shock front at the selected simulation times are shown in Fig. 9. In Fig. 9(a), the detonation wave has not reached the edge of the explosive at 5 cm, and CH_4 and NH_3 are produced among the detonation product species. The structure of the thin air

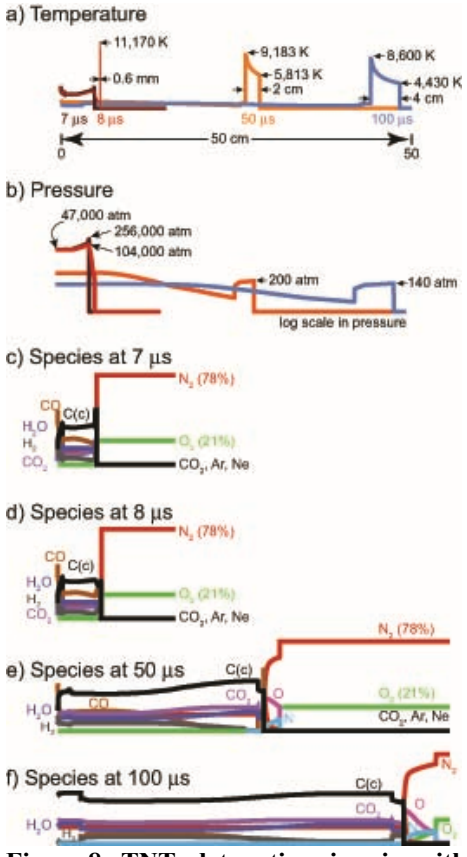

Figure 8. TNT detonation in air with profiles of a) temperature, b) pressure, and species at c) 7 μs, d) 8 μs, e) 50 μs, and f) 100 μs.

shock is shown in Fig. 9(b). Free radicals, N and O from the dissociation of N_2 and O_2, respectively, are formed. At these high temperatures, electrons are stripped from N and NO, forming N^+ and NO^+. In Fig. 9(c), the concentration of the N radical decays more than an order of magnitude across the thin shock. Since the temperatures within the shock fall below 6000 K, according to Fig. 7, the ion concentrations vanish. The same conclusion can be drawn for Fig. 9(d), where one boundary drops to 4,430 K. Since CTH does not model mixing of materials within a computational cell, the TNT and air within the mixed cells at the shock front profiles presented in Fig. 9 are not burned, and TIGER calculates the equilibrium concentration of the reacted products in those cells. At longer times, mixing is expected to be important. For 500 g spheres of TNT, as reported by Kovar, turbulent mixing begins near 200 μs.

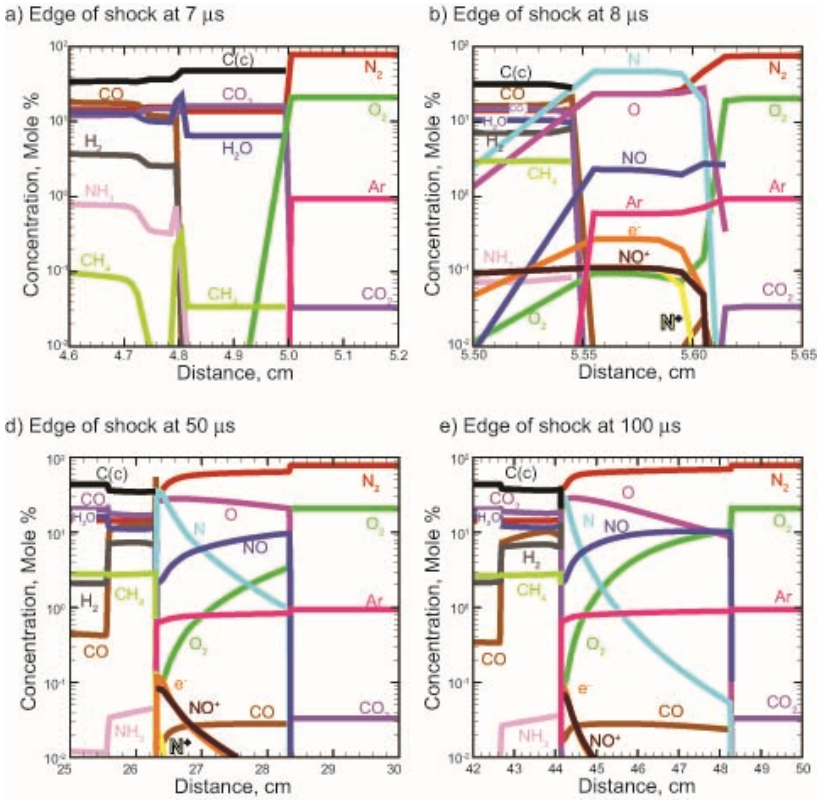

Figure 9. TNT detonation in air with profiles of the species a) w ithin the explosive at 7 μs, and within the air shock at b) 8 μs, c) 50 μs, and d) 100 μs.

E. 3D CTH-TIGER Predictions

The 1D CTH-TIGER simulations of the previous section provided sufficient resolution within a thin shock structure to gain new understanding on a simple test case that could be repeated multiple times for refining the code interfacing methodology. Three-dimensional simulations using the same cylindrical shaped charge provided significantly larger data sets for testing our methodology, and represented a more realistic test case, given that many problems of interest have complicated geometries, and of sufficient size to necessitate high performance parallel computing. In fact, efficiently initializing a CFD code with partitioned data sets from a parallel simulation is still an outstanding research challenge. CTH calculations of a top-initiated right circular cylinder using a 45 cm x 45 cm x 45 cm computational domain with a uniform cell size of 0.2 cm are shown in Fig. 10. Although these problems were fairly straightforward, ensuring that CTH-TIGER converged for 11M individual data points required revisions to solvers, database parameters, and other code improvements. Results from these 16-node simulations are given in

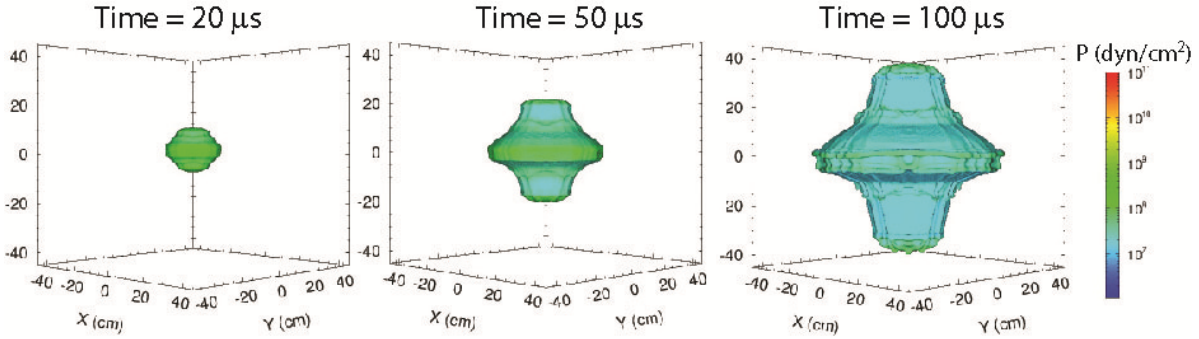

Figure 10. 3D CTH simulations TNT expansion products from cylindrical charge detonation at various times.

Fig. 11. Here, the computational species fields are presented on data planes. The shape of the shock wave structure is as expected from the previous 2D results. At 20 μs, where the data are extracted, the peak temperature in the shock front is at approximately 7000 K. Solid carbon C(c) is distributed in the TNT detonation products, while the free radicals and electrons are only present in the air shock front.

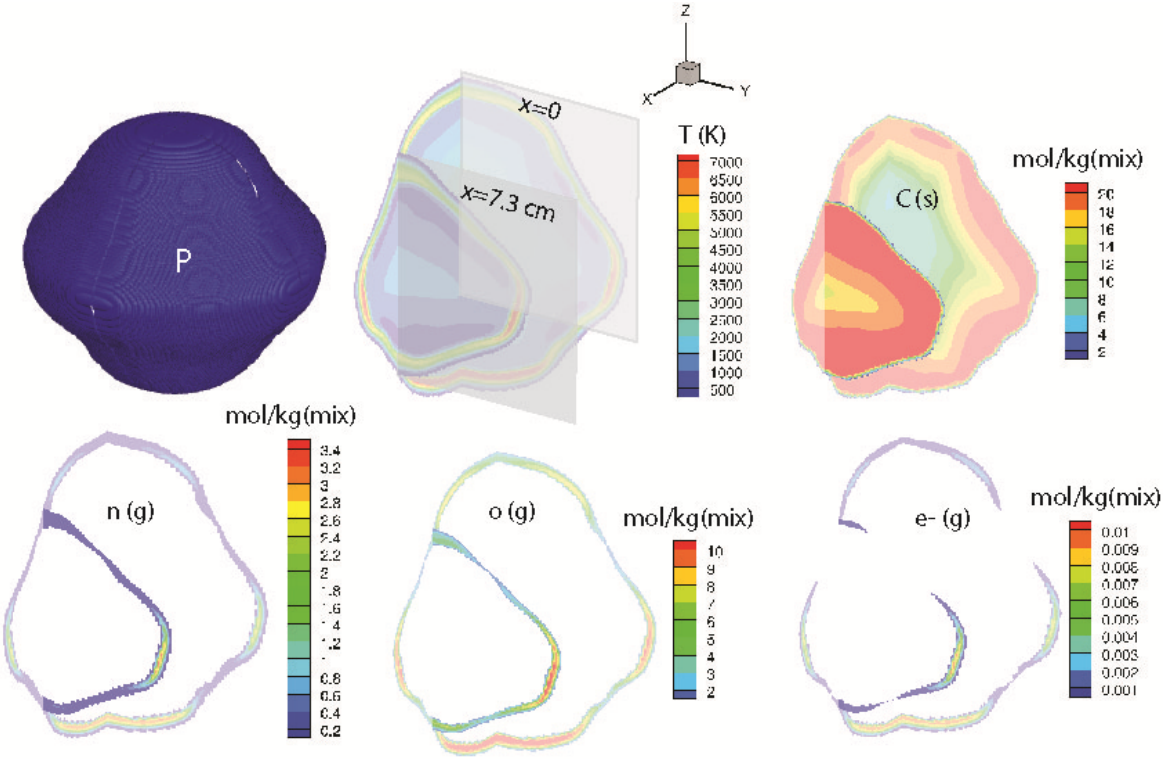

Figure 11. Prediction of spatial distributions of pressure, temperature, and species following detonation of a cylindrical charge of TNT in air using CTH.

IV. Conclusion

A major outcome of this paper was the development of a new tool, CTH-TIGER, to permit transitioning from a detonation to an air shock, providing spatial species concentrations that could be passed to a combustion fluid dynamics code for initializing a simulation of secondary detonation products combustion. An integrated code approach is needed to address this complex problem, and this work serves as a significant advancement of previous methods using a single code. Research still needs to be completed to pass large data sets from parallel computation. Future work will be extending this methodology beyond systems with two materials such as an explosive and air, but to also include metal particle combustion.

Acknowledgments

Sandia National Laboratories is a multi-program laboratory managed and operated by Sandia Corporation, a wholly owned subsidiary of Lockheed Martin Corporation, for the U.S. Department of Energy's National Nuclear Security Administration under contract DE-AC04-94AL85000.

References

[1]Trélat, S. , Sochet, I., Autrusson, B.,Cheval, K., and Loiseau, O., "Impact of a Shock Wave ona Structure on Explosion at Altitude," *Journal of Loss Prevention in the Process Industries*, Vol. 20, 2007, pp. 509-516.

[2]Makhviladze, G. M., and Yakush, E., "Blast Waves and Fireballs from Bursts of Vessels with Pressure-liquefied Hydrocarbons," *Proceedings of the Combustion Institute*, Vol. 29, 2002, pp. 313-320.

[3]Roy, G. D. , Frolov, S. M., Borisov, A. A., and Netzer, D. W., "Pulse Detonation Propulsion: Challenges, Current Status, and Future Perspective," *Progress in Energy and Combustion Science*, Vol. 30, 2004, pp. 545-672.

[4]Horie, Y. (ed.), *Shock Wave Science and Technology Reference Library, Vol. 3: Solids II*, Springer-Verlag, Berlin, 2009.

[5]Zhang, F. (ed.), *Shock Wave Science and Technology Reference Library, Vol. 6: Detonation Dynamics*, Springer-Verlag, Berlin, 2012.

[6]Kuo, K. K., *Principles of Combustion*, John Wiley & Sons, New York, 1986.

[7]Ornellas, D. L., "The Heat and Products of Detonation of Cyclotetramethylenetetranitramine, 2,4,6-Trinitrotolune, Nitromethane, and Bis[2,2-dinitro-2-fluoroethyl]formal" *The Journal of Physical Chemistry*, Vol. 72, No. 7, 1968, pp. 2390-2394.

[8]Kuhl, A. L., and Reichenbach, H., "Combustion Effects in Confined Explosions," *Proceedings of the Combustion Institute*, Vol. 32, 2009, pp. 2291-2298.

[9]Kuhl, A. L., Bell, J. B., Beckner, V. E., and Reichenbach, H., "Gasdynamic Model of Turbulent Combustion in TNT Explosions," *Proceedings of the Combustion Institute*, Vol. 33, 2011, pp. 2177-2185.

[10]Kovar, F. R., Trigger, K. R., Guymon, L. G., and Harvey, J. R., "High Explosive Detonations in Varying Oxygen Atmospheres," *AIP Conference Proceedings*, Vol. 78, 1982, pp. 563-567.

[11]McGlaun, J. M., Thompson, S. L., and Elrick, M. G., "CTH: A Three-Dimensional Shock Wave Physics Code," *International Journal of Impact Engineering*, Vol. 10, 1990, pp. 351-360.

[12]Cowperthwaite, M., and Zwisler, W. H., "TIGER Computer Program Documentation," SRI Publication No. Z106, Menlo Park, CA, 1973.

[13]Hobbs, M. L., Brundage, A. L., and Yarrington, C. D., "JCZS2i: An Improved JCZ Database for EOS Calculations at High Temperature and Pressure," *Fifthteenth International Detonation Symposium*, San Francisco, CA, 2014 (submitted for publication).

[14]Bennett, B. I., Johnson, J. D., Kerley, G. I., and Rood, G. T., "Recent Developments in the Sesame Equation-of-State Library," Los Alamos Scientific Laboratory, Rept. LA-17130, 1978.

[15]Kerley, G. I., "CTH Reference Manual: The Equation of State Package," Sandia National Laboratories, Rept. SAND91-0334, 1991.

[16]Tecplot 360 Data Format Guide, Ver. 2008, Tecplot, Inc., Bellevue, WA, 2008.

[17]van Leer, B., "Towards the Ultimate Conservative Difference Scheme" *Journal of Computational Physics*, Vol. 23, 1977, pp. 276-299.

[18]Lee, E. L., Hornig, H. C., and Kury, J. W., "Adiabatic Expansion of High Explosive Detonation Products," Lawrence Radiation Laboratory, Rept. UCRL-505422, 1968.

[19]Zel'dovich, Y. B., and Raizer,Y. P., *Physics of Shock Waves and High-Temperature Hydrodynamic Phenomena, Vol. II*, edited by W. D. Hayes and R. F. Probstein, Academic Press, New York, 1967.

[20]McBride, B. J., and Gordon, S., "Computer Program for Calculation of Complex Chemical Equilibrium Compositions and Applications II. Users Manual and Program Description," NASA Reference Publication 1311, NASA Lewis Research Center, Cleveland, OH, 1996.